1 **Supplementary information to:**

2

3 RECKLEEN: a lambda Red/CRISPR-Cas9 based single plasmid platform for fast, 4 efficient, markerless, and scarless genome editing in *Klebsiella pneumoniae*.

5 Eslam M. Elsayed[1,2,3], Daniel Stukenberg[1,#], Bernd Schmeck[1,4,5], and Anke Becker[1,2,*]

6 [1]Center for Synthetic Microbiology, Philipps-Universität Marburg, Marburg, Germany

7 [2]Department of Biology, Philipps-Universität Marburg, Marburg, Germany

8 [3]Department of Microbiology and Immunology, Faculty of Pharmacy, Zagazig University, Zagazig, Egypt

9 [4]Institute for Lung Research, Universities of Giessen and Marburg Lung Center, German Center for Lung
10 Research (DZL), Philipps-University Marburg, Marburg, Germany

11 [5]Department of Medicine, Pulmonary and Critical Care Medicine, University Medical Center Marburg,
12 Universities of Giessen and Marburg Lung Center, Philipps-University Marburg, Marburg, Germany

13 [*]For correspondence: anke.becker@synmikro.uni-marburg.de

14 #Current address: Department of Biology, Technical University Darmstadt, Darmstadt, Germany

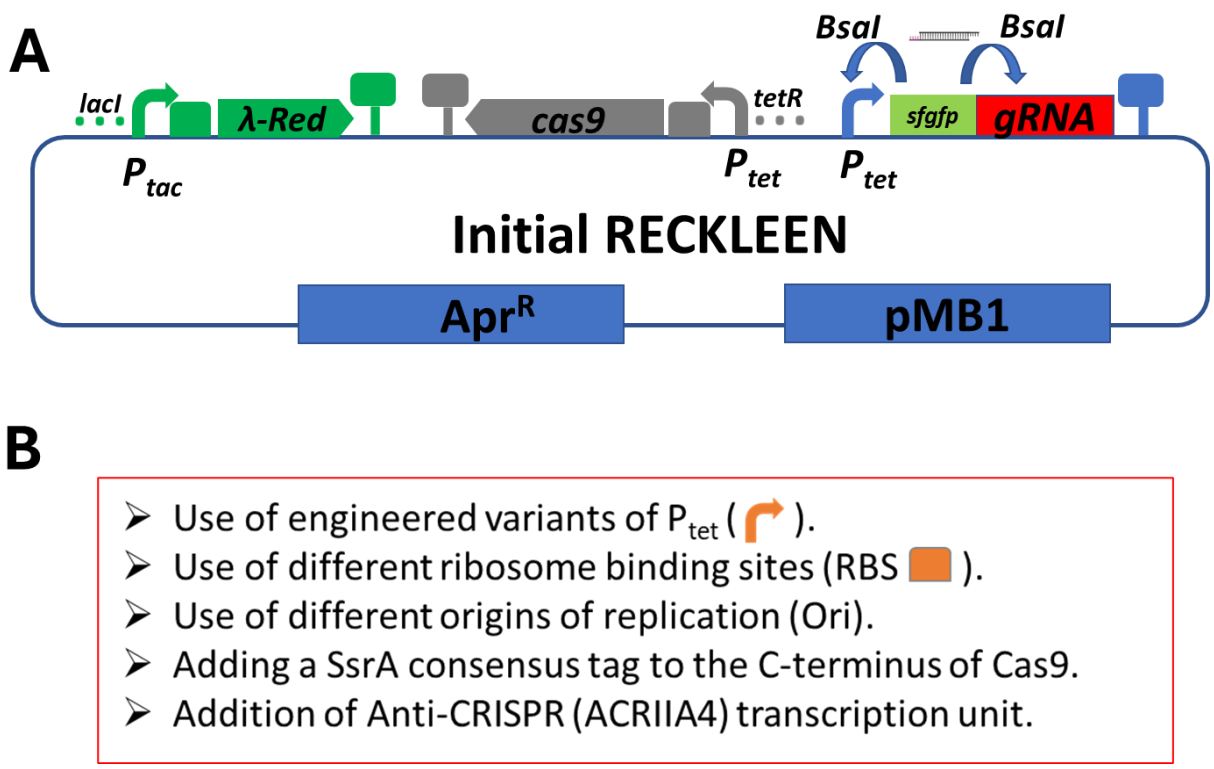

Supplementary Figure 1. A) Schematic design of the initial plasmid constructed to prototype the RECKLEEN system in *Kp*. The plasmid carries three different transcriptional units: the lambda Red operon (*gam, exo, beta*) under control of the inducible P_{tac} promoter, as well as the *cas9* and *sgRNA* transcription units, both under control of the inducible P_{tet} promoter. The vector backbone carries the *lacI* and *tetR* genes encoding the transcription regulators of these promoters and an apramycin resistance gene marker and a pMB1 origin of replication. This plasmid can be customized by replacing a sfGFP transcription unit in front of the *sgRNA* scaffold-encoding sequence with a 20-nt guide spacer sequence through Golden Gate assembly using the BsaI restriction enzyme. **B)** Applied strategies to address the possible toxic effects of a hypothesized leaky expressing the CRISPR/Cas9 part of the RECKLEEN system targeting the genomic sequence. Anti-CRISPR (AcrIIA4) mitigates the lethal effect of the CRISPR/Cas9 part of the RECKLEEN system and enables electroporation of the plasmids with *sgRNA* targeting the genomic sequence of *Kp*. The plasmid construct has been redesigned to contain an *acrIIA4* transcription unit, constitutively expressed under the control of the constitutive promoter J23100.

Supplementary Figure 2. Evaluation of *wzi* deletion in *Kp* ATCC700721. A) Colony PCR results demonstrating the deletion of the *wzi* gene using primers that bind approximately 500 bp outside the deleted region. Lane M represents the marker; WT corresponds to the wild-type strain, which serves as a positive control for the unmodified *wzi* locus. All relevant experiments are available in Supplementary Data 3. **B)** Sanger sequencing of PCR products confirmed the deletion of *wzi*. Sequencing was performed by Microsynth Seqlab, using PCR fragments and primers binding upstream or downstream of the targeted modification. In total, six PCR fragments, including both biological and technical replicates, were sequenced. The wild-type (WT) sequence is shown alongside the sequences of the replicates. Alignment of sequencing files was conducted using SnapGene® 5.0.8, with screenshots provided to illustrate the deletion of the *wzi* coding sequence. All relevant sequencing files are available in the Supplementary Data 6.

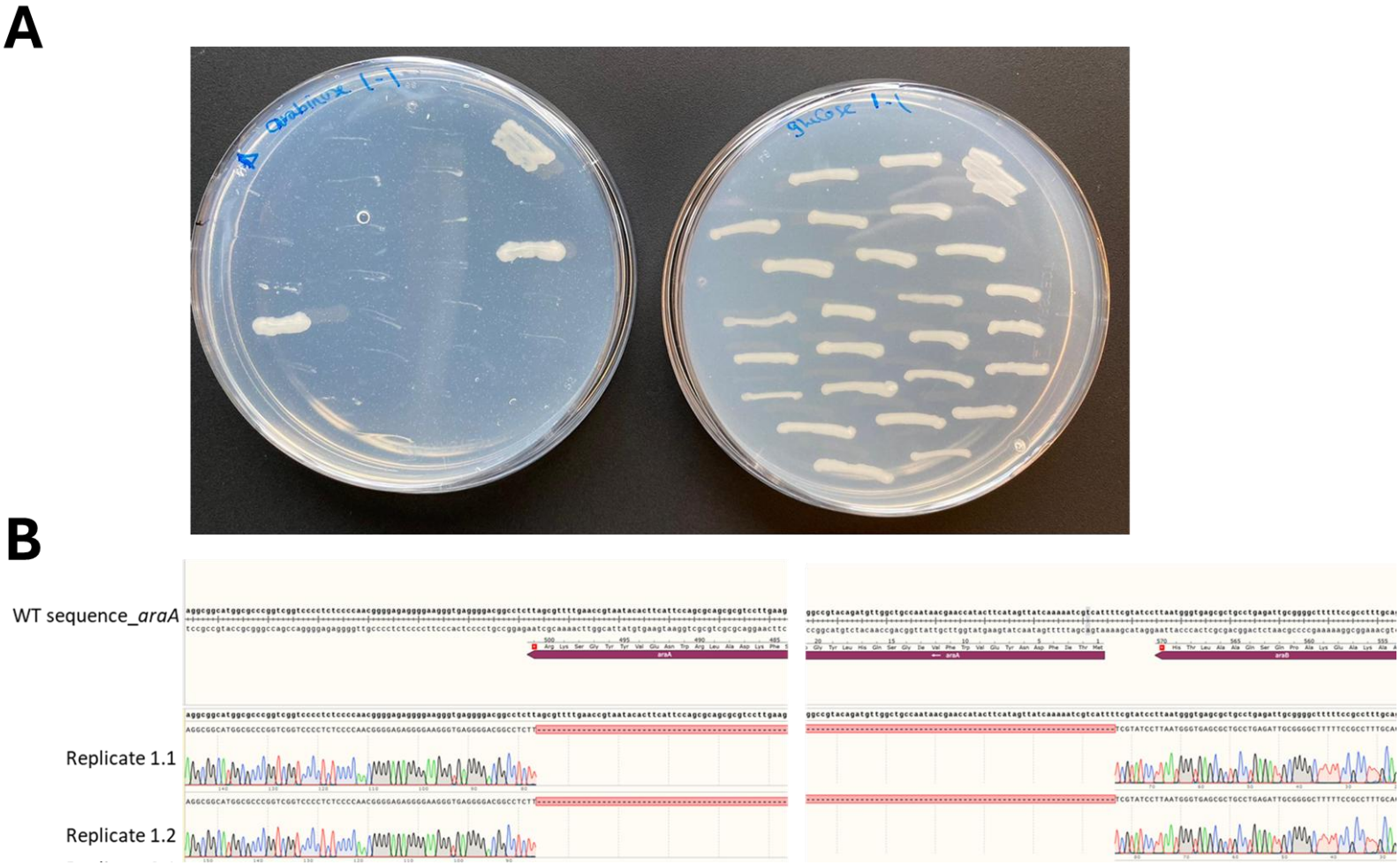

Supplementary Figure 3. Evaluation of *araA* deletion. A) Phenotypic characterization of *araA* deletion. The deletion of the *araA* gene was screened phenotypically by streaking the obtained colonies on M9 minimal medium agar plates with either glucose or the alternative carbon source (arabinose in this case). Colonies that grew on M9 plates with glucose but failed to grow on arabinose plates were classified as successfully edited. All relevant experiments are available in Supplementary Data 4. **B)** Sanger sequencing of PCR products confirmed the deletion of *araA*. Sequencing was performed by Microsynth Seqlab, using PCR fragments and primers binding upstream or downstream of the targeted modification. In total, six PCR fragments, including both biological and technical replicates, were sequenced. The wild-type (WT) sequence is shown alongside the sequences of the replicates. Alignment of sequencing files was conducted using SnapGene® 5.0.8, with screenshots provided to illustrate the deletion of the *araA* coding sequence. All relevant sequencing files are available in Supplementary Data 6.

A

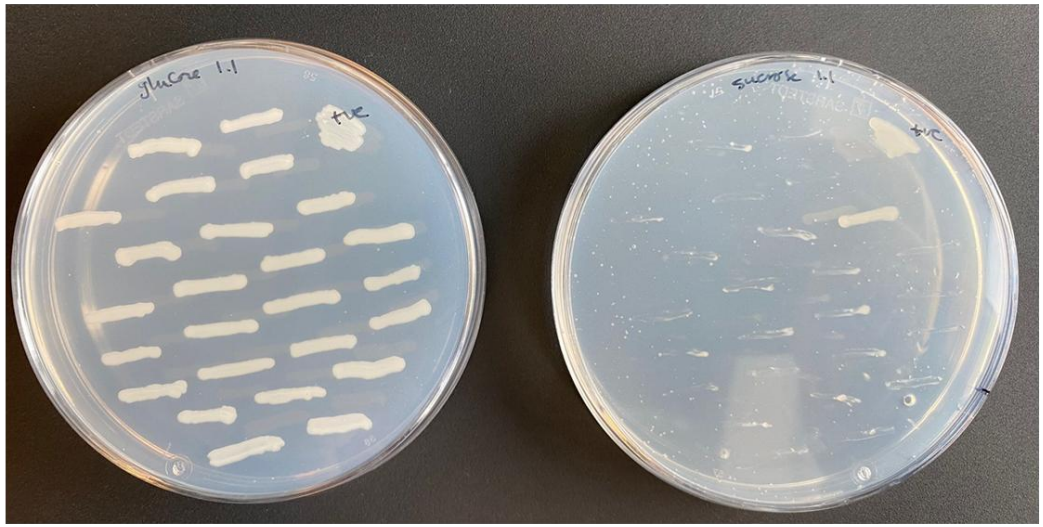

B

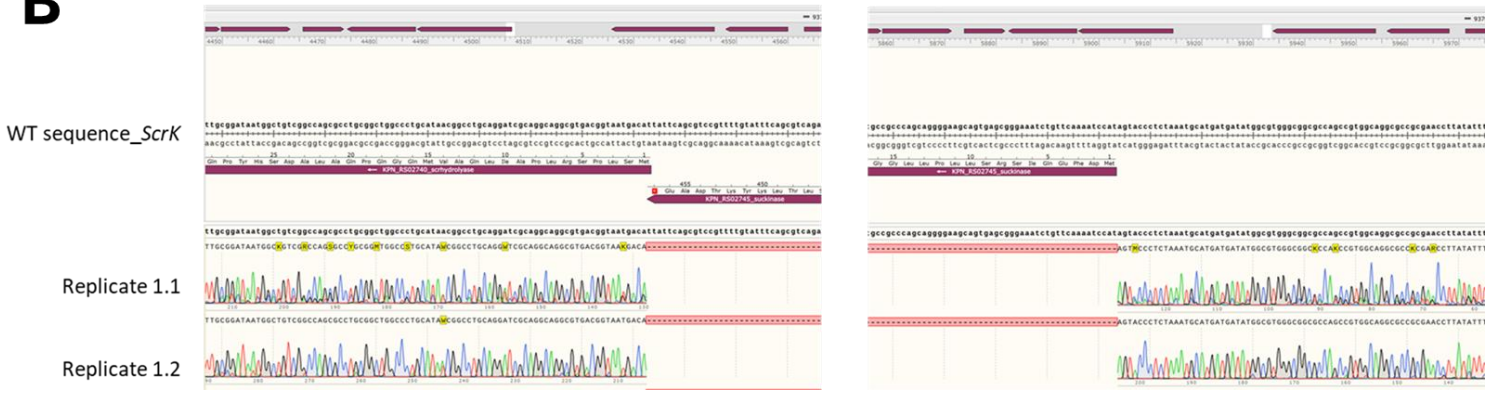

Supplementary Figure 4. Evaluation of *scrK* deletion. A) Phenotypic characterization of *scrK* deletion. The deletion of the *scrK* gene was screened phenotypically by streaking the obtained colonies on M9 minimal medium agar plates with either glucose or the alternative carbon source (sucrose in this case). Colonies that grew on M9 plates with glucose but failed to grow on sucrose plates were classified as successfully edited. All relevant experiments are available in Supplementary Data 4. **B)** Sanger sequencing of PCR products confirmed the deletion of *scrK*. Sequencing was performed by Microsynth Seqlab, using PCR fragments and primers binding upstream or downstream of the targeted modification. In total, six PCR fragments, including both biological and technical replicates, were sequenced. The wild-type (WT) sequence is shown alongside the sequences of the replicates. Alignment of sequencing files was conducted using SnapGene® 5.0.8, with screenshots provided to illustrate the deletion of the *scrK* coding sequence. All relevant sequencing files are available in Supplementary Data 6.

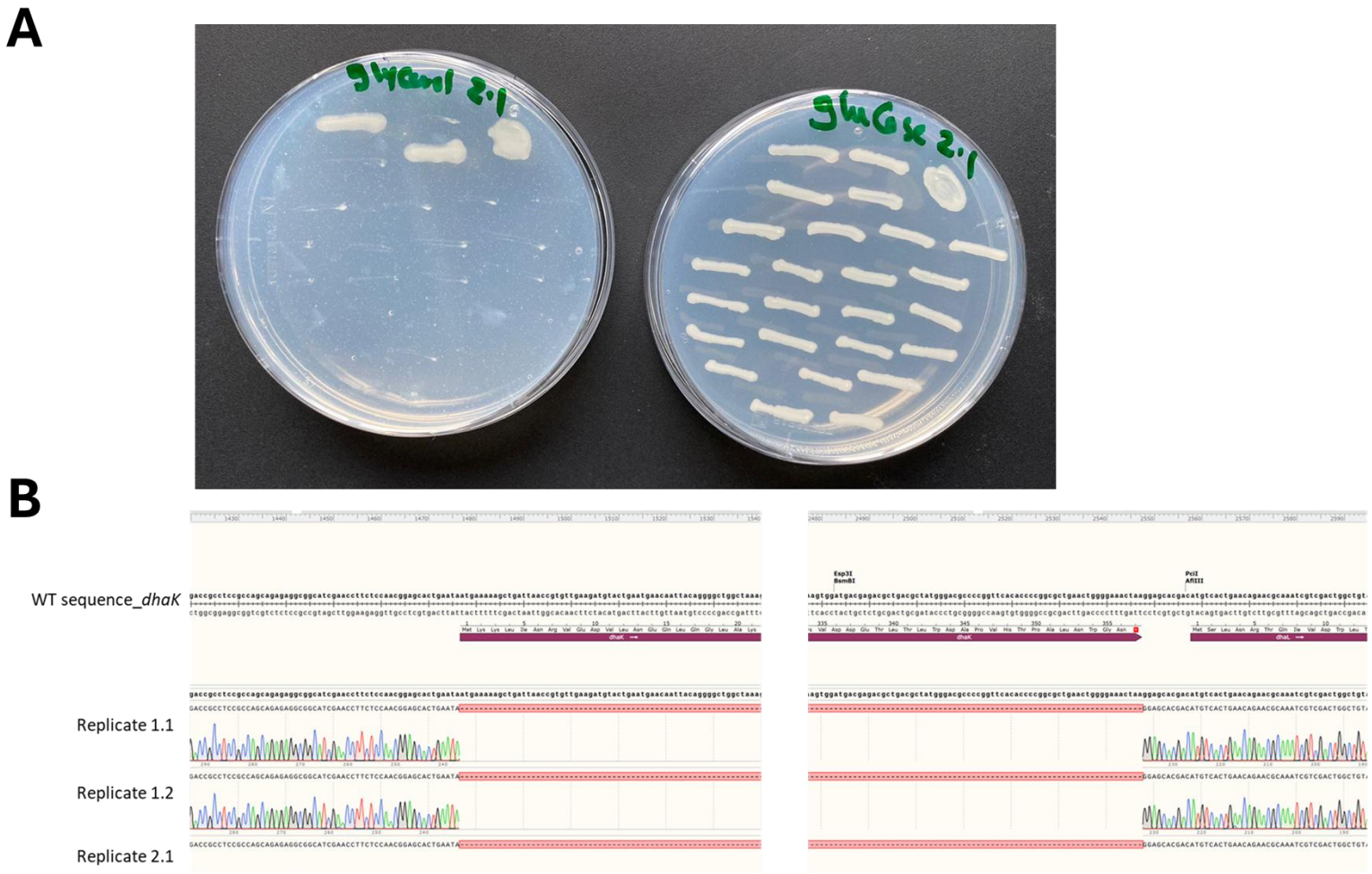

Supplementary Figure 5. Evaluation of *dhaK* deletion. A) Phenotypic characterization of *dhaK* deletion. The deletion of the *dhaK* gene was screened phenotypically by streaking the obtained colonies on M9 minimal medium agar plates with either glucose or the alternative carbon source (glycerol in this case). Colonies that grew on M9 plates with glucose but failed to grow on glycerol plates were classified as successfully edited. All relevant experiments are available in Supplementary Data 4. **B)** Sanger sequencing of PCR products confirmed the deletion of *dhaK*. Sequencing was performed by Microsynth Seqlab, using PCR fragments and primers binding upstream or downstream of the targeted modification. In total, six PCR fragments, including both biological and technical replicates, were sequenced. The wild-type (WT) sequence is shown alongside the sequences of the replicates. Alignment of sequencing files was conducted using SnapGene® 5.0.8, with screenshots provided to illustrate the deletion of the *dhaK* coding sequence. All relevant sequencing files are available in Supplementary Data 6.

A

B

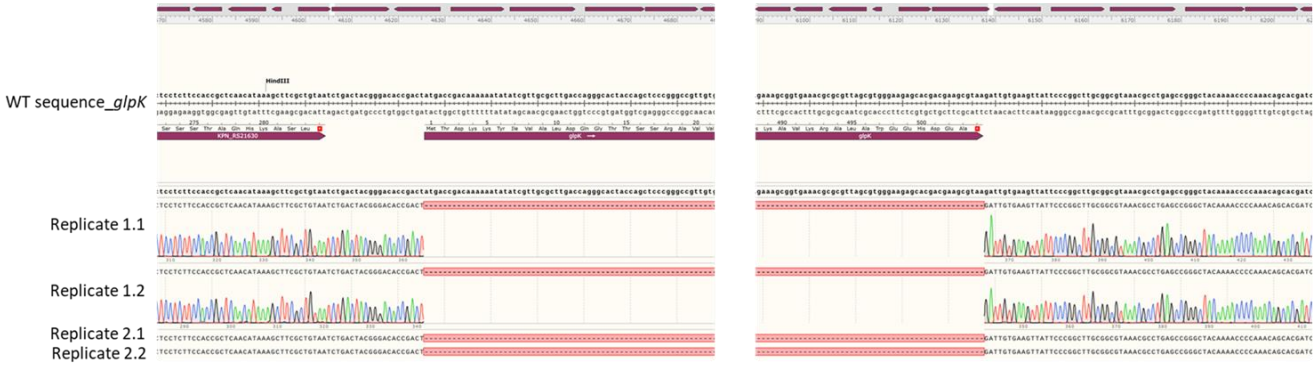

Supplementary Figure 6. Evaluation of *glpK* deletion. A) Phenotypic characterization of *glpK* deletion. The deletion of the *glpK* gene was screened phenotypically by streaking the obtained colonies on M9 minimal medium agar plates with either glucose or the alternative carbon source (glycerol in this case). Colonies that grew on M9 plates with glucose but failed to grow on glycerol plates were classified as successfully edited. All relevant experiments are available in Supplementary Data 4. **B)** Sanger sequencing of PCR products confirmed the deletion of *glpK*. Sequencing was performed by Microsynth Seqlab, using PCR fragments and primers binding upstream or downstream of the targeted modification. In total, six PCR fragments, including both biological and technical replicates, were sequenced. The wild-type (WT) sequence is shown alongside the sequences of the replicates. Alignment of sequencing files was conducted using SnapGene® 5.0.8, with screenshots provided to illustrate the deletion of the *glpK* coding sequence. All relevant sequencing files are available in Supplementary Data 6.

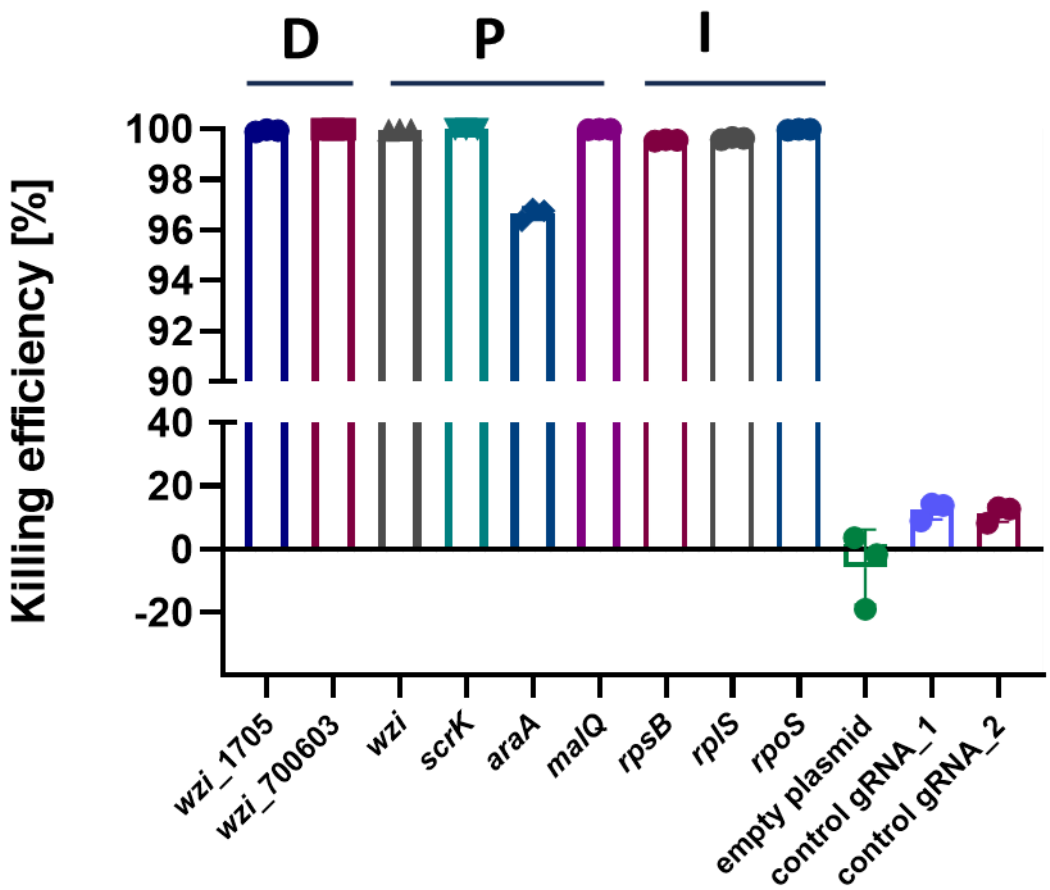

Supplementary Figure 7. Killing efficiency for various *sgRNA* for the deletion (D), point mutation (P), and DNA integration (I) of different target genes. The killing efficiency was measured after induction with ATc. The killing efficiency was calculated as follows: $Killing\ efficiency\ [\%] = 1 - \frac{\frac{CFU}{mL}\ in\ presence\ of\ inducer(\ with\ counterselection)}{\frac{CFU}{mL} in absence\ of\ inducer\ (without\ counterselection)} * 100$ to measure the percentage of killed cells upon induction of the system. Data represents the mean of three biological replicates and the error bars represent the standard deviation from the mean.

Supplementary Figure 8. Evaluation of *wzi*_C66A point mutation. Sanger sequencing was performed through Microsynth Seqlab using PCR fragments and a primer binding upstream or downstream of the respective modification. In total, six different PCR fragments were sequenced. The wild-type (WT) sequence is shown alongside the sequences of the replicates for comparison. All sequencing alignments were performed using SnapGene® 5.0.8, with screenshots demonstrating the successful incorporation of the C66A point mutation. Additionally, guanine (G57) of *wzi* was edited into cytosine (C) as a silent alanine mutation besides the previously designed point mutation to overcome the mismatch repair mechanism. The sequencing files are provided in Supplementary Data 6.

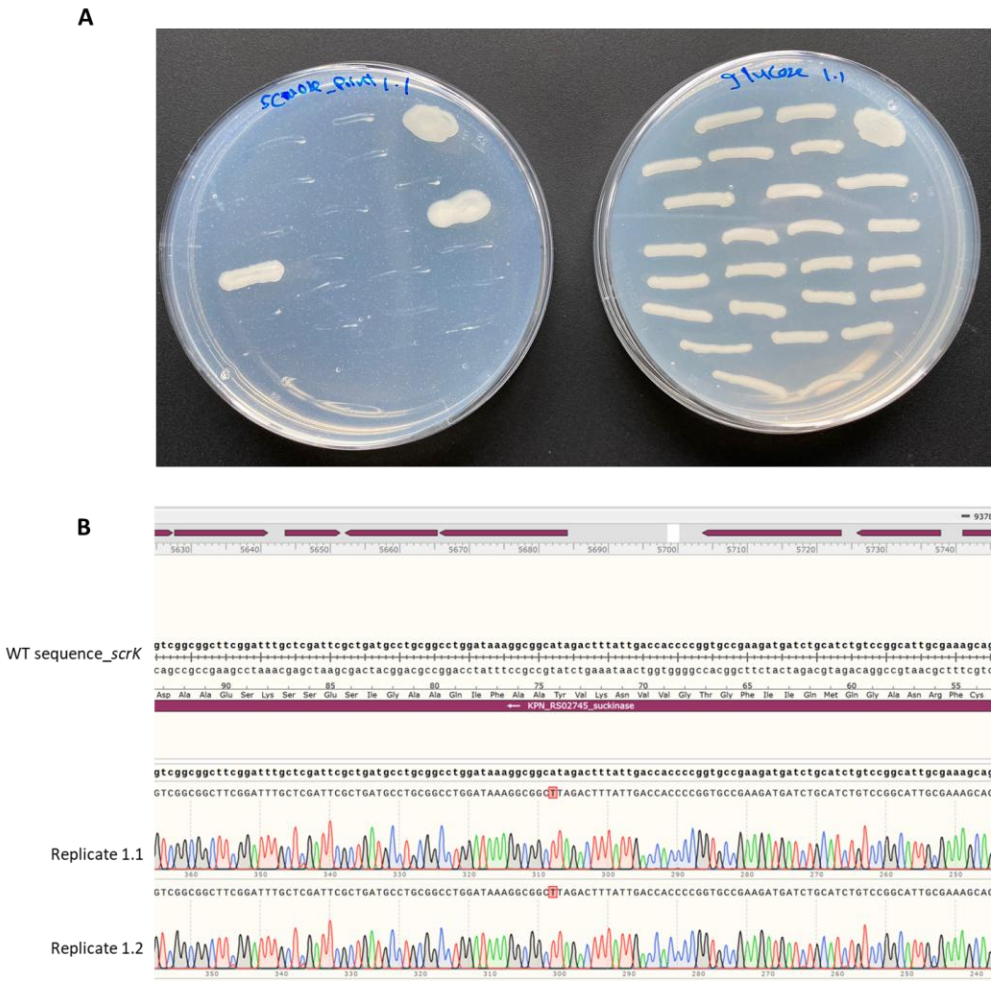

Supplementary Figure 9. Evaluation of *scrK*_T222A point mutation. A) Phenotypic characterization of *scrK*_T222A point mutation. The point mutation of the *scrK* gene was screened phenotypically by streaking the obtained colonies on M9 minimal medium agar plates with either glucose or the alternative carbon source (sucrose in this case). Colonies that grew on M9 plates with glucose but failed to grow on sucrose plates were classified as successfully edited. All relevant experimental data are available in Supplementary Data 4. **B)** Sanger sequencing of PCR products confirmed the point mutation of *scrK*. Sequencing was performed by Microsynth Seqlab, using PCR fragments and primers binding upstream or downstream of the targeted modification. In total, six PCR fragments, including both biological and technical replicates, were sequenced. The wild-type (WT) sequence is shown alongside the sequences of the replicates. Alignment of sequencing files was conducted using SnapGene® 5.0.8, with screenshots provided to illustrate the point mutation. All relevant sequencing files are available in Supplementary Data 6.

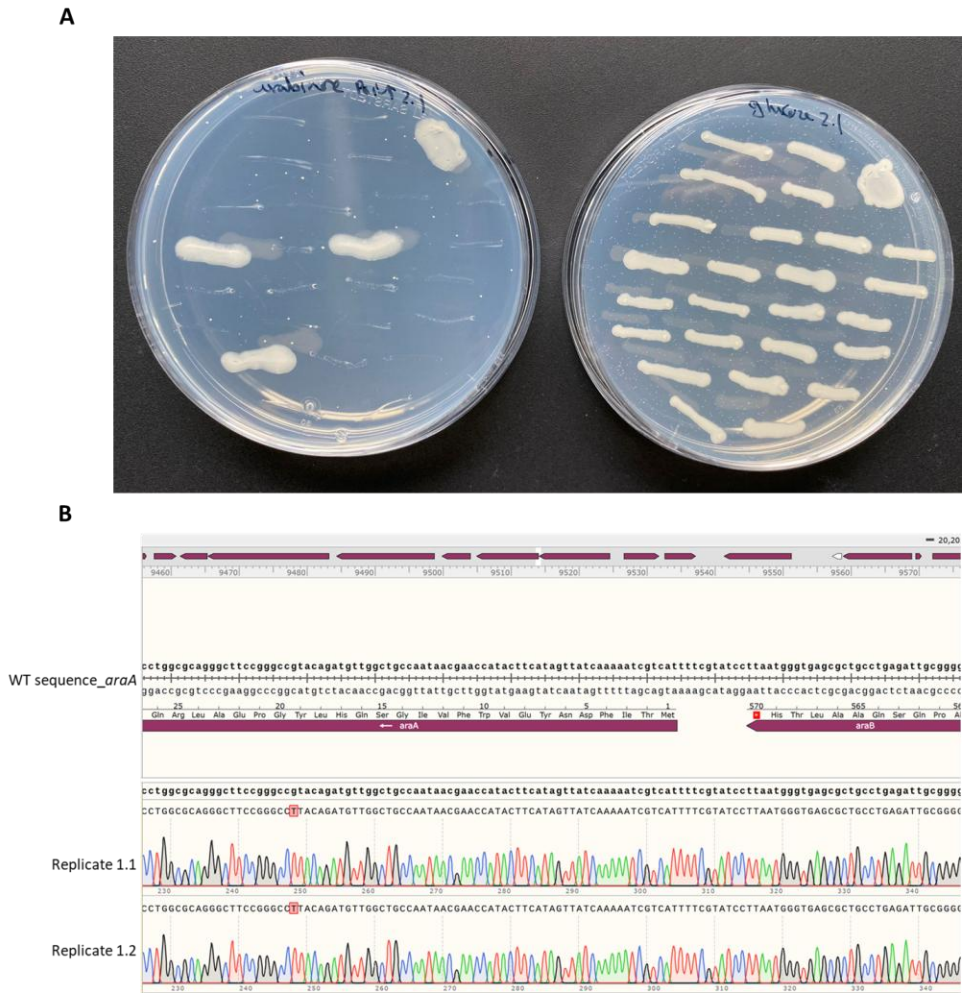

Supplementary Figure 10. Evaluation of *araA*_C57A point mutation. A) Phenotypic characterization of *araA*_C57A point mutation. The point mutation of the *araA* gene was screened phenotypically by streaking the obtained colonies on M9 minimal medium agar plates with either glucose or the alternative carbon source (arabinose in this case). Colonies that grew on M9 plates with glucose but failed to grow on arabinose plates were classified as successfully edited. All relevant experimental data are available in Supplementary Data 4. **B)** Sanger sequencing of PCR products confirmed the point mutation of *araA*. Sequencing was performed by Microsynth Seqlab, using PCR fragments and primers binding upstream or downstream of the targeted modification. In total, six PCR fragments, including both biological and technical replicates, were sequenced. The wild-type (WT) sequence is shown alongside the sequences of the replicates. Alignment of sequencing files was conducted using SnapGene® 5.0.8, with screenshots provided to illustrate the point mutation. All relevant sequencing files are provided in Supplementary Data 6.

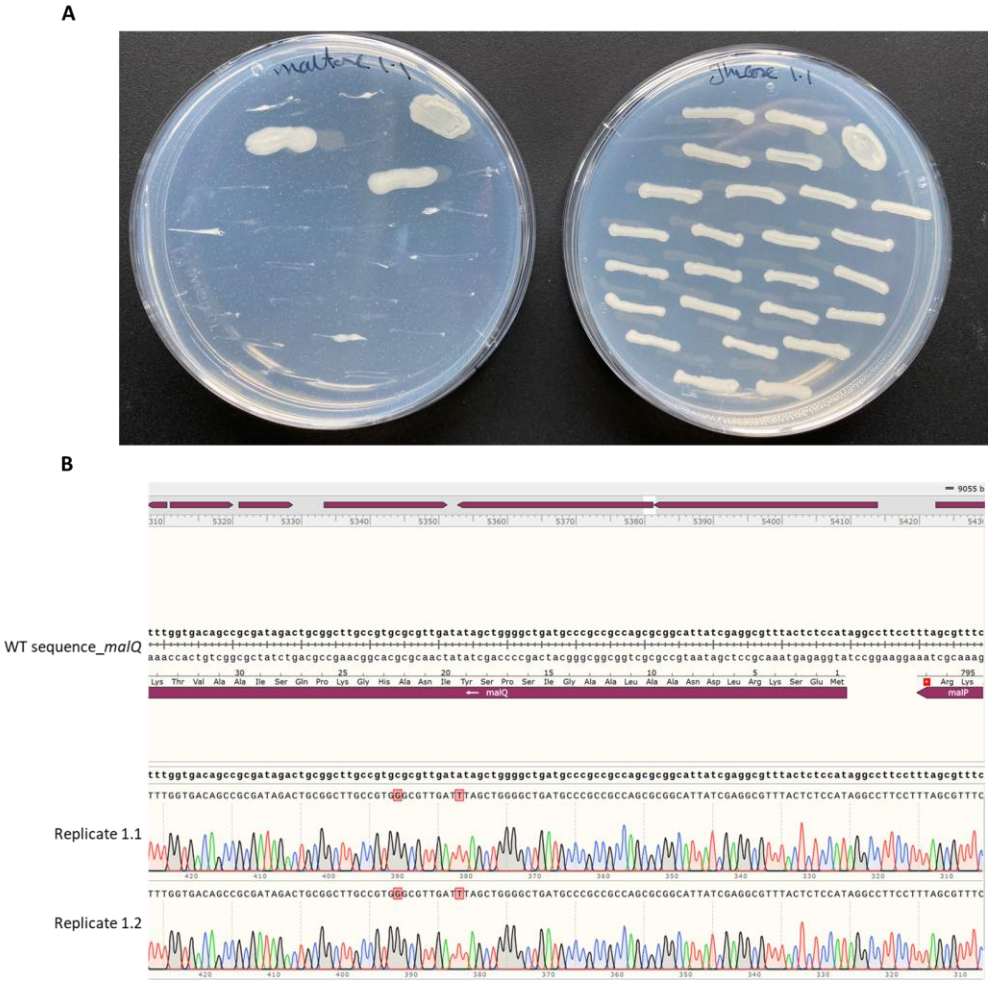

Supplementary Figure 11. Evaluation of *malQ*_T57A point mutation. A) Phenotypic characterization of *malQ*_T57A point mutation. The point mutation of the *malQ* gene was screened phenotypically by streaking the obtained colonies on M9 minimal medium agar plates with either glucose or the alternative carbon source (maltose in this case). Colonies that grew on M9 plates with glucose but failed to grow on maltose plates were classified as successfully edited. All relevant experimental data are available in Supplementary Data 4. **B)** Sanger sequencing of PCR products confirmed the point mutation of *malQ*. Sequencing was performed by Microsynth Seqlab, using PCR fragments and primers binding upstream or downstream of the targeted modification. In total, six PCR fragments, including both biological and technical replicates, were sequenced. The wild-type (WT) sequence is shown alongside the sequences of the replicates. Alignment of sequencing files was conducted using SnapGene® 5.0.8, with screenshots provided to illustrate the point mutation. Additionally, Guanine (G66) of malQ was edited into Cytosine (C) as a silent alanine mutation besides the previously designed point mutation to overcome the mismatch repair mechanism. The sequencing files are provided in Supplementary Data 6.

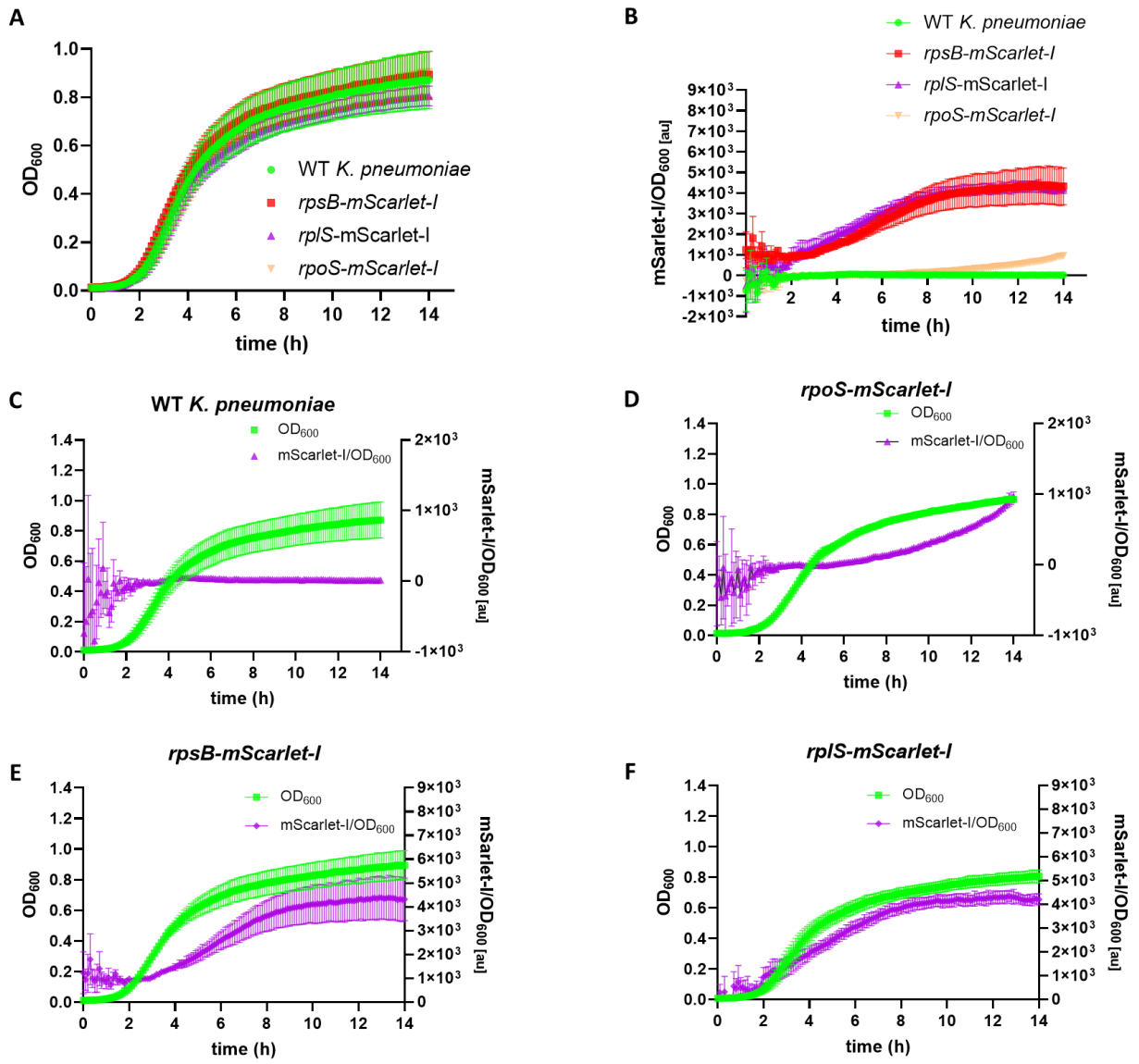

Supplementary Figure 12. Evaluation of DNA integrations. A) Growth Curves of WT *Kp* and strains with integrated mScarlet-I fused to the 3' end of *rpsB, rplS*, and *rpoS.* The integration of the mScarlet-I didn't affect the growth of the *Kp* strains**. B)** Normalized m-Scarlet-I signal of WT *Kp* and strains with integrated mScarlet-I fused to the 3' end of *rpsB, rplS*, and *rpoS.* **C)** Growth curve (shown in green) and normalized mScarlet-I signal (shown in violet) of WT *Kp***. D)** Growth curve (shown in green) and normalized mScarlet-I signal (shown in violet) of *Kp* with integrated mScarlet-I fused to the 3' end of *rpoS.* **E)** Growth curve (shown in green) and normalized mScarlet-I signal (shown in violet) of with integrated mScarlet-I fused to the 3' end of *rpsB.* **F)** Growth curve (shown in green) and normalized mScarlet-I signal (shown in violet) of with integrated mScarlet-I fused to the 3' end of *rplS*. Data represents the mean of three biological replicates and two independent experiments, and the error bars represent the standard deviation from the mean. Similar expression patterns of the two ribosomal genes (*rpsB* and *rplS*) during the bacterial growth. Both have been significantly upregulated after 2 hrs of growth. This upregulation continued till 8 hours with a steady state increase. Then, it reached a stable level after 8 hrs. On the other hand, the stress sigma factor *rpoS* was significantly upregulated during the stationary phase after almost 8 hrs of bacterial growth.

Supplementary Figure 13. Evaluation of *mScarlet-I integration fusion to* the 3' end of *rplS*. Sanger sequencing was performed through Microsynth Seqlab using PCR fragments and a primer binding upstream or downstream of the respective modification. In total, six different PCR fragments were sequenced. The expected sequence is shown alongside the sequences of the replicates for comparison. All sequencing alignments were performed using SnapGene® 5.0.8, with screenshots demonstrating the successful DNA integration. The sequencing files are provided in Supplementary Data 6.

Supplementary Figure 14. Evaluation of *mScarlet-I* integration fusion to the 3' end of *rpsB*. Sanger sequencing was performed through Microsynth Seqlab using PCR fragments and a primer binding upstream or downstream of the respective modification. In total, six different PCR fragments were sequenced. The expected sequence is shown alongside the sequences of the replicates for comparison. All sequencing alignments were performed using SnapGene® 5.0.8, with screenshots demonstrating the successful DNA integration. The sequencing files are provided in Supplementary Data 6.

Supplementary Figure 15. Evaluation of *mScarlet-I* integration fusion to the 3' end of *rpoS*. Sanger sequencing was performed through Microsynth Seqlab using PCR fragments and a primer binding upstream or downstream of the respective modification. In total, six different PCR fragments were sequenced. The expected sequence is shown alongside the sequences of the replicates for comparison. All sequencing alignments were performed using SnapGene® 5.0.8, with screenshots demonstrating the successful DNA integration. The sequencing files are provided in Supplementary Data 6.

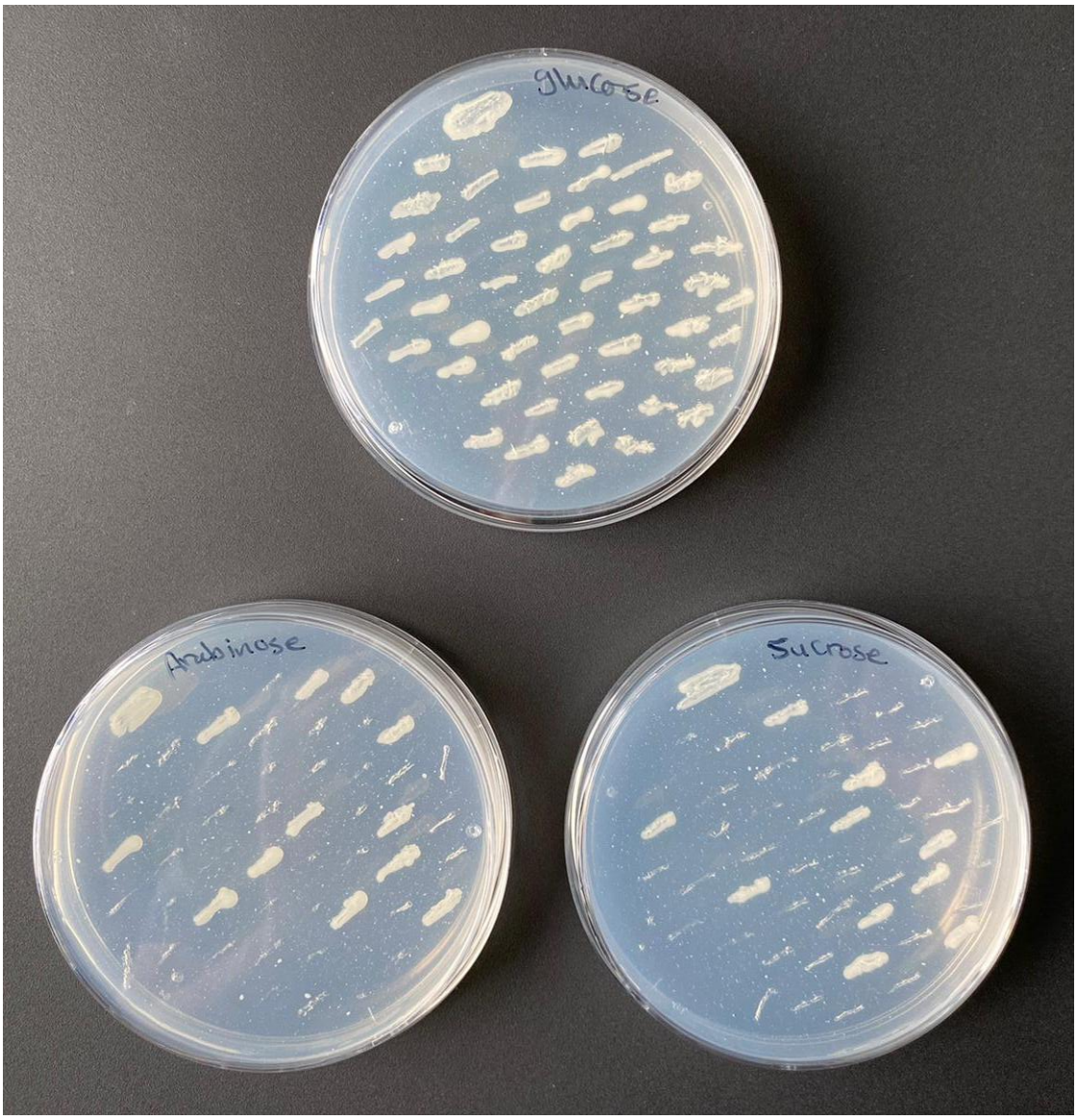

Supplementary Figure 16. Evaluation of multi-target deletions of *araA* and *scrK* using REKLEEN 3 platform. Phenotypic characterization of *araA* and *scrK* deletions. The deletion was screened phenotypically by streaking the obtained colonies on M9 minimal medium agar plates with either glucose or the alternative carbon source (arabinose and sucrose in this case). Colonies that grew on M9 plates with glucose but failed to grow on the respective secondary carbon source plates were classified as successfully edited. In total, fifty colonies were tested. Sanger sequencing was then harnessed to confirm the deletion of the two genes. The sequencing files are provided in supplementary Data 6. The desired deletion of the target genes was detected in 72% of the randomly selected colonies. Around 4% of the selected colonies had *araA* but not *scrK* deleted, while 6% showed deletion of *scrK* but not *araA*.

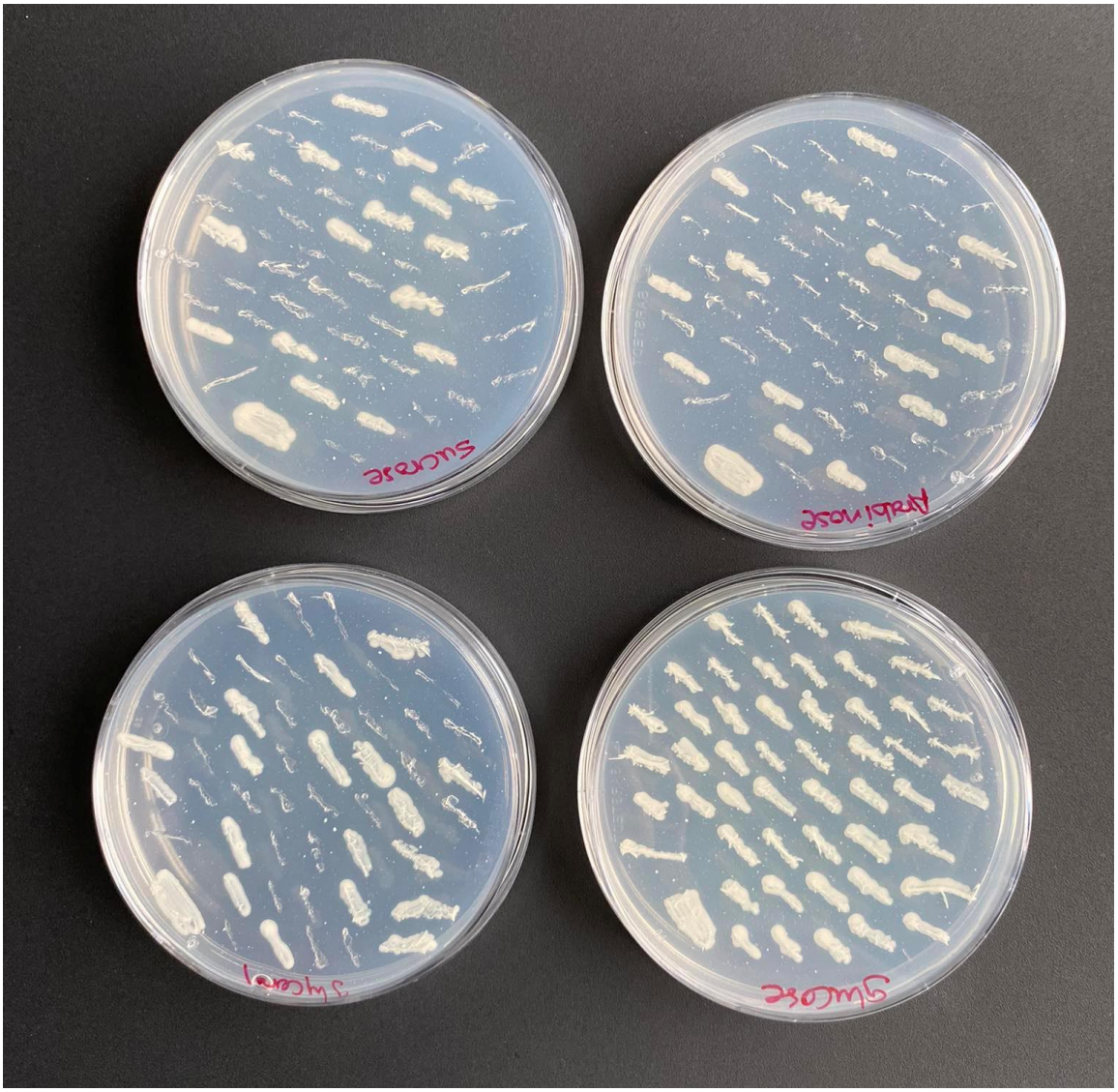

Supplementary Figure 17. Evaluation of multi-target deletions of *araA, dhaK* and *scrK* using REKLEEN 3 platform. Phenotypic characterization of *araA, dhaK* and *scrK* deletions. The deletion was screened phenotypically by streaking the obtained colonies on M9 minimal medium agar plates with either glucose or the alternative carbon source (arabinose, glycerol, and sucrose in this case). Colonies that grew on M9 plates with glucose but failed to grow on the respective secondary carbon source plates were classified as successfully edited. In total, fifty colonies were tested. Sanger sequencing was then harnessed to confirm the deletion of the two genes. The sequencing files are provided in Supplementary Data 6. The desired deletion of the target genes was detected in 54% of fifty randomly selected colonies. Around 6% of the selected colonies showed a single deletion (2% for *araA* and 4% for *scrK*). Around 16% of the selected colonies showed deletion of two genes but not the third one (8%, 6%, and 2% showed deletion of *araA & scrK, araA & dhak, and scrK & dhak*, respectively).

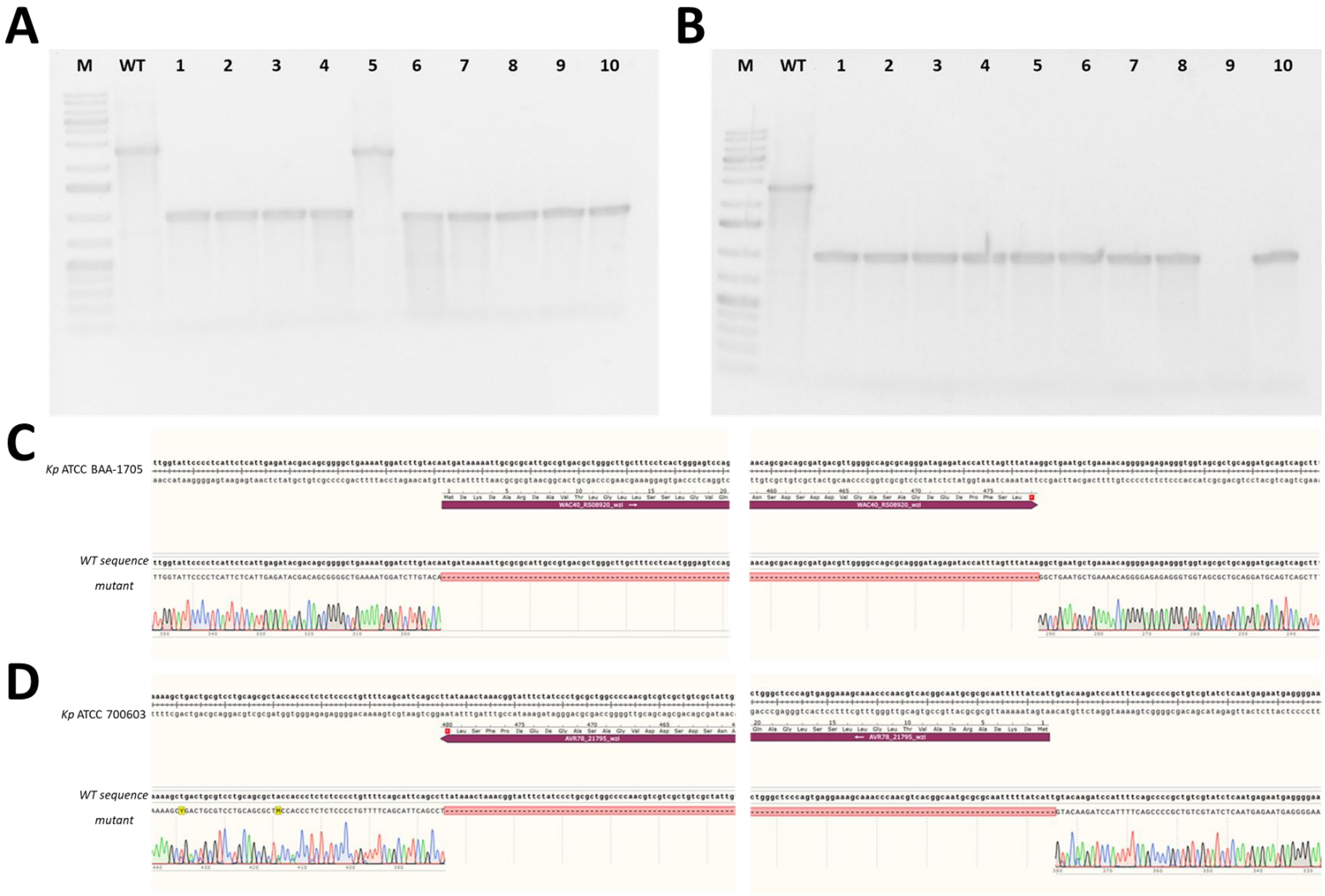

Supplementary Figure 18. Evaluation of *wzi* deletion in MDR *Kp* strains, *Kp* ATCC BAA-1705 **(A)** and *Kp* ATCC 700603 **(B)**. Colony PCR results of demonstrating the deletion of the *wzi* gene using primers that bind approximately 500 bp outside the deleted region. Lane M represents the marker; WT corresponds to the wild-type strain, which serves as a positive control for the unmodified *wzi* locus. **C) & D)** Evaluation of *wzi* deletion in *Kp* ATCC BAA-1705 and ATCC 700603 by Sanger sequencing. Screenshots showing alignment of sequencing files with the Kp genome sequence by SnapGene® 5.0.8. The sequencing files are provided in Supplementary Data 6.

158 **Supplementary Tables provided in Supplementary Data 2**

159 Supplementary Table 1: Assembly of plasmids used in this study.

Supplementary Table 2: Bacterial strains used in this study.

160 Supplementary Table 3: Oligonucleotides used to assemble *sgRNA* sequences.

161 Supplementary Table 4: Oligonucleotides used for the construction of dDNA template plasmids.

162 Supplementary Table 5: Oligonucleotides to generate dDNA fragments from dDNA template plasmids.

163 Supplementary Table 6: ssDNA oligonucleotides to generate dDNA fragments.